CHEMISTRY OF MATERIALS

Article

pubs.acs.org/cm

Sacrificial Templates for Galvanic Replacement Reactions: Design Criteria for the Synthesis of Pure Pt Nanoshells with a Smooth Surface Morphology

Kyle D. Gilroy, Pouyan Farzinpour, Aarthi Sundar, Robert A. Hughes, and Svetlana Neretina*

College of Engineering, Temple University, Philadelphia, Pennsylvania 19122, United States

Supporting Information

ABSTRACT: The galvanic replacement of sacrificial templates offers one of the most synthetically viable approaches for generating platinum-based nanostructures with impressive catalytic activity. Here, we present template design criteria for the synthesis of morphologically smooth platinum nanoshells which undergo minimal alloying with the template material. The criteria is founded on comparisons of nanoshells derived from reacting substrate-immobilized templates of silver, lead, copper, nickel, and cobalt with aqueous H_2PtCl_6. It is shown that template-surface modifications are the primary mode by which smooth Pt nanoshells are obtained, with template composition playing a secondary role. The degree of alloying is strongly dependent upon whether the template applies tensile or compressive heteroepitaxial strains to the depositing nanoshell. On the basis of these findings, we propose a mechanistic framework and an overall strategy for the synthesis of advanced templates for substrate-based galvanic replacement reactions.

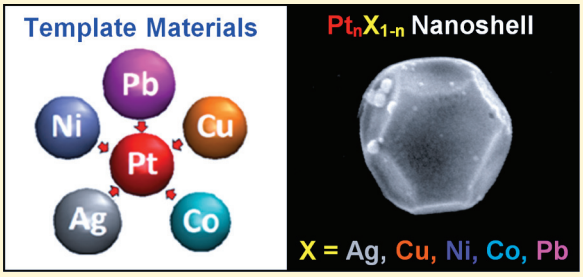

INTRODUCTION

Galvanic replacement reactions offer a synthetically powerful approach for transforming solid sacrificial templates into hollow metal nanostructures.[1] Reactions yielding Pt nanoshells are of intense interest due to the anticipated enhancements to the catalytic activity derived from high surface area nanostructures with morphologies tailored to optimize specific rates of reaction.[2−5] Ag nanostructures are, by far, the most commonly used sacrificial templates for galvanic replacement reactions due to a relatively low electrochemical potential[1] and a colloidal chemistry that is both rich and well-established.[2,6,7] Templates with nanosphere,[8,9] nanocube,[10−13] nanoplate,[14] nanorod,[15] and nanowire[16−18] configurations have all yielded nanoshell geometries when reacted with various platinum reagents (e.g., H_2PtCl_6, K_2PtCl_4, Na_2PtCl_4, and $Na_2Pt(OH)_6$). Such structures have consistently demonstrated enhanced catalytic activity when compared to commercially available catalysts. Despite this success, a number of issues have arisen. Ag templates consistently yield bimetallic Pt−Ag nanoshells with surface morphologies which are much rougher and more fragile than those obtained by reacting identical templates with reagents of other precious metals. In addition, the bimetallic nature reduces the catalytic activity[11,19] and the rough surface morphology precludes the possibility of generating highly faceted nanoshells with distinctive catalytic properties.[2,20] Proposed explanations for the poor morphology include the following: (i) the 3.5% lattice mismatch between Pt and Ag, (ii) the poor miscibility of the Ag−Pt binary system at low temperatures, and (iii) the reaction byproduct Cl^- which initiates the growth of AgCl on the template surface.[21]

While Ag is the predominant template material, its inadequacies have motivated studies targeting the synthesis of superior nanoshells through the use of alternate template materials and/or chemical modifications to the surface of existing templates. The galvanic replacement of Co[22,23] and Ni[24,25] templates both yield porous shells composed of many small interconnected lobes. Hollow nanoboxes with a similar surface morphology were derived from Cu_2O nanocube templates.[26] Noteworthy, however, is that the synthesis gave rise to nanostructures composed of pure Pt which, because they lack surface agents, present clean catalytic surfaces. Cu nanowire templates yield Pt nanotubes with significant Cu alloying,[5,27] but where the surface morphology, while still exhibiting some roughness, is superior to all of the aforementioned template materials. Te nanowire templates, when reacted in ethylene glycol, yielded smooth nanotubes, but where unsatisfactory morphologies are obtained when carrying out the same reaction in water or ethanol.[28] Noteworthy is that Pt nanoshells with smooth and continuous walls have been achieved through modifications to the template surface prior to the onset of the galvanic replacement reaction. Ag nanowire and nanocube templates with a thin AgCl surface layer give rise to smooth Pt nanotubes[16] and nanoboxes,[21] respectively. Morphological improvements are also observed for Ni nanowire templates when exposed to an H_2SO_4 pretreatment.[29] Also of note is the morphological control asserted for the

Received: April 18, 2014
Published: May 5, 2014

   dx.doi.org/10.1021/cm501418d | Chem. Mater. 2014, 26, 3340−3347

Table 1. Template Material Parameters of Relevance to Pt-Based Galvanic Replacement Reactions

element (ion)	redox $E°$ (V vs standard hydrogen electrode)[a]	replacement ratio (X:Pt)	crystal structure	lattice constant (Å)	induced force in platinum layer
Pb (Pb^{2+})	−0.13[b]	2:1	fcc	4.951	tension
Ag (Ag^{+})	0.80[b]	4:1	fcc	4.085	tension
Pt (Pt^{4+})	0.74[c]	N/A	fcc	3.942	N/A
Ni (Ni^{2+})	−0.24[b]	2:1	fcc	3.524	compression
Cu (Cu^{2+},Cu^{+})	0.34, 0.52[b]	2:1, 4:1	fcc	3.615	compression
Co (Co^{2+})	−0.28[b]	2:1	hcp	2.507, 4.070	compression[d]

[a]Conditions for 25 °C and 1 atm. [b]Reference 36. [c]Reference 23. [d]Based on comparisons of interatomic distances in the close-packed plane.

galvanic replacement of highly faceted Pd templates when exposed to Br^{-} during the replacement reaction.[30]

Studies performed to date have definitively established the importance of template design in determining the product of galvanic replacement reactions directed toward the formation of Pt nanostructures with hollowed morphologies. The varied nature of the numerous synthetic protocols does, however, make it difficult to separate out the role of the template's elemental makeup from confounding factors which arise when comparing reactions with dissimilar reagents, concentrations, temperatures, and durations carried out on templates with different sizes, shapes, faceting, and surface agents. Previously, we demonstrated the synthesis of substrate-based Au−Ag nanoshells and nanocages[31,32] using sacrificial templates derived from solid-state dewetting[33] and related techniques.[34,35] Such techniques, which rely on the agglomeration of thin metal films at elevated temperatures, provide a straightforward route for obtaining crystalline template materials from a wide variety of elements. Once formed, template surfaces can be modified through the physical vapor deposition of a thin layer of a second element over their surface. Such surface modifications have the potential to (i) alter the heteroepitaxial relationship between the depositing shell and template, (ii) diminish nanoshell alloying, and (iii) limit the exposure of the underlying template to both the reagent and reaction byproducts. Here, we demonstrate the galvanic replacement of both bare and surface-modified Ag, Pb, Cu, Ni, and Co templates with aqueous H_2PtCl_6, where all of the templates are of similar size and shape and exposed to comparable reaction conditions. The product of the reaction, for all bare templates, is an alloyed nanoshell with a rough morphology, but where surface modifications to certain templates yield a near-pure product with a smooth and continuous surface. On the basis of these findings, we present design criteria for template architectures able to promote the formation of smooth nanoshells with minimal alloying.

■ EXPERIMENTAL SECTION

Chemicals and Materials. Sputter targets of Ag, Pb, Cu, Ni, Co, Au, and Pt were cut from 0.5 mm thick foils (Alfa Aesar, Ward Hill, MA, USA) with 99.99+% purity. Bi targets were cut from a rod (ESPI Metals, Ashland, OR, USA) with 99.999% purity. Polished (0001)-oriented sapphire (MTI Corporation, Richmond, CA, USA) and Si_3N_4 TEM support films (Electron Microscopy Sciences, Hatfield, PA, USA) were used as substrates. Templates were formed in either ultra high purity Ar or a 1:9 H_2:Ar mixture. Nanoshell synthesis utilized chloroplatinic acid hydrate ($H_2PtCl_6{\cdot}xH_2O$, 99.9% trace metals basis, Sigma-Aldrich, St. Louis, MO, USA), deionized Milli-Q water (18.2 MΩ·cm at 25 °C), nitric acid (2.0 N, HNO_3), and hydrochloric acid (HCl), the latter two from Alfa Aesar. All chemicals were used as received.

Synthesis of Sacrificial Templates. Templates of Ag, Pb, Cu, Ni, and Co were formed as periodic arrays of nearly identical structures or as randomly positioned structures with a substantial size distribution using substrate-based techniques described in detail elsewhere.[33−35] All template materials (Ag, Pb, Cu, Ni, and Co) and passivation layers were sputter-deposited using a Model 681 Gatan High Resolution Ion Beam Coater. The layer thicknesses and heating regimens used to obtain the various template materials are summarized in the Supporting Information (Table S1). All templates were assembled in a Lindberg Blue M tube furnace under a flowing gas ambient (65 sccm) where a dedicated quartz tube was used for each template material to avoid cross-contamination. The gas ambient was Ar for Ag and Cu, but where sensitivity to surface oxidation necessitated the introduction of 10% H_2 (balance argon) for Pb, Ni, and Co. The assembly processes were carried out on 8 × 8 × 0.5 mm (0001)-oriented sapphire substrates for all template materials. When possible, they were also carried out on Si_3N_4 TEM support films to simplify TEM sample preparation. These support films could not, however, withstand the processing temperatures associated with the fabrication of Ni and Co templates. The templates were then left bare or were, alternatively, modified by sputter coating a 3 nm thick layer of either Pt, Au, or Cu over their entire surface. The coatings are smooth and follow the contours of the template.[32] Such modifications were carried out immediately after the assembled templates were removed from the tube furnace to minimize surface oxidation. The electrochemical potential ($E°$), replacement ratio, crystal structure, lattice constant, and anticipated elastic strain imposed on the depositing nanoshell due to lattice mismatch with the template for all of the aforementioned materials is summarized in Table 1.

Synthesis of Nanoshells. Galvanic replacement reactions were carried out in a 10 mL beaker which was cleaned with aqua regia and then thoroughly rinsed with DI water. Both the bare and surface-modified templates were reacted immediately following their synthesis. Reactions proceeded through the immersion of a template-covered substrate into a 10 mL solution of aqueous H_2PtCl_6 heated to 90 °C. The concentration of the aqueous solution was either 50 or 100 μM depending on whether the expected Pt replacement ratio is 1:4 (i.e., Ag, Cu) or 1:2 (i.e., Pb, Ni, Co), respectively. After the templates are allowed to react for 10 min, the substrate is slowly pulled from the solution with Teflon tweezers and immediately placed into a beaker containing 2 N nitric acid for 5 min. This procedure removes precipitates from the substrate surface, but does not noticeably affect the formed nanoshells. The sample is then gently rinsed with DI water and allowed to dry. All concentrations were reduced by a factor of 2 when reacting templates formed on Si_3N_4 support films or as periodic arrays

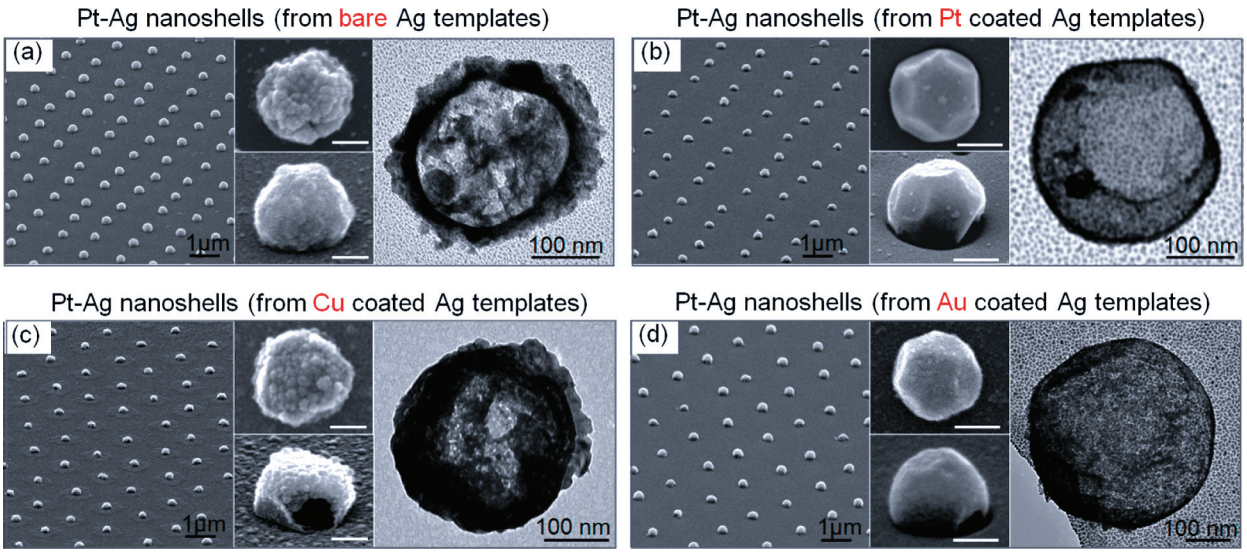

Figure 1. Images of hollow Pt−Ag nanoshells as periodic arrays and as individual structures which were derived from (a) Ag templates, and Ag templates coated with a 3 nm thick layer of (b) Pt, (c) Cu, and (d) Au. The three leftmost SEM images in each frame show a periodic array of nanoshells and individual structures imaged from a top and 65° tilted view (scale bar for insets is 100 nm). For each frame the rightmost image is a TEM micrograph of a hollow nanoshell which was peeled from the substrate surface, a process which left two of the structures inverted (Figures 1a,b). The smaller particles coating each of the TEM grids are a remnant of the nanostructure peeling process.[32]

to compensate for the smaller amount of template material being reacted. The templates were then transformed into nanoshells through galvanic replacement in aqueous H_2PtCl_6. Noteworthy is the fact that all of these reactions were carried out in the absence of capping agents. Such agents prevent the agglomeration of solution-dispersed templates, but often complicate reaction pathways[9,21] and/or result in diminished catalytic activity.[37,38]

Characterization. Transmission electron microscopy (TEM) images were obtained using a JEOL JEM-1400 TEM equipped energy-dispersive X-ray spectroscopy (EDS) analyzer. Selected area electron diffraction patterns and the associated diffraction patterns were obtained using an FEI Tecnai 12T TEM. Scanning electron microscopy (SEM) was performed using either an FEI Quanta 400 Environmental scanning electron microscope (ESEM) or a 450 FEG ESEM.

RESULTS AND DISCUSSION

Role of Template Surface Passivation. Figure 1 shows a comparison of SEM images between nanoshells derived from periodic arrays of Ag templates formed on sapphire and identical arrays, modified by sputter coating a 3 nm thick layer of either Pt, Au, or Cu over their entire surface. The templates were approximately 270 nm in diameter where the majority of the structures have either a [110] or [111] orientation.[32] The templates have a rounded morphology, but where weak {111} and {100} faceting is observed.[39] Apart from the fact that the Pt−Ag nanoshells are substrate-immobilized, those obtained from bare templates (Figure 1a) show all the hallmarks characteristic of this galvanic replacement reaction. This includes a rough surface morphology and a bimetallic composition with near equal atomic percentages of Pt and Ag. TEM images of nanoshells that were peeled off the substrate surface in a manner which often leaves them inverted on a TEM grid[32] reveal that the structures are, indeed, hollow. In stark contrast, Ag templates passivated with a thin layer of Pt prior to reaction yield exceedingly smooth ultrathin nanoshells (Figure 1b). The structures typically take on a nanohut[31] geometry, characterized by a downward facing shell with a single prominent opening at the base. EDS measurements show a Pt:Ag ratio of 50:50. The observed thickness is in line with expectations which take into account the expected 4:1 Ag:Pt replacement ratio, a sputter-deposited thickness of 3 nm, and the observed degree of alloying. Of note is the unusually high diameter-to-thickness ratio of 40 exhibited by these nanoshells, a value attributable to both the large template sizes accessible in substrate-based galvanic replacement reactions and the robustness of these structures. Periodic arrays of nanoshells with a smooth morphology were also derived from Au-passivated Ag templates (Figure 1d). Cu-passivated templates, however, yield rough nanoshells, similar to those derived from bare Ag templates (Figure 1c). It is, however, noted that the Cu layer will be partially consumed in the galvanic replacement process.[27]

Several immediate conclusions can be drawn from a comparison of the reactions products derived from templates with various surface layers. The fact that smooth shells are obtained for Ag templates coated with either Pt or Au argues against lattice mismatch being the likely source of the poor surface morphology typically expressed by Pt−Ag nanoshells. The Au coating is particularly revealing since the Au−Pt combination has an almost identical lattice mismatch to the Ag−Pt combination (3.5% vs 3.3%), but is, nevertheless, still able to yield smooth nanoshells. Poor miscibility between Pt and Ag is also an unlikely source. In fact, the materials seem to readily alloy for the temperatures and length scales of relevance to nanoshells as is evidenced by the insensitivity of the nanoshell composition to HNO_3 exposure, an acid which attacks Ag, but not Pt. Direct evidence for Pt−Ag alloying using X-ray diffraction and electron diffraction is provided by Zhang et al.[21] and Kim et al.,[9] respectively. The fact that the Cu-coated templates yield rough morphologies demonstrates that the coating process is not, in and of itself, responsible for the smooth morphologies. The trend is, instead, one where coatings that are unable to undergo direct oxidation and dissolution result in smooth morphologies while highly reactive

dx.doi.org/10.1021/cm501418d | Chem. Mater. 2014, 26, 3340−3347

surfaces (i.e., uncoated templates or coatings with a low reduction potential) yield rough morphologies. This result points toward surface passivation as being the crucial factor in regulating the surface morphology of the resultant nanoshell. In this scenario, dissolution can only occur from a point on the surface where the passivation layer is breached.

Elemental and morphological characterization of nanoshells derived from bare and surface-passivated templates were carried out using Ag templates assembled directly on TEM grids equipped with Si_3N_4 support films. Nanoshells produced in this manner greatly simplify TEM sample preparation. Because the amorphous surface of Si_3N_4 is incapable of supporting heteroepitaxy, such templates form in numerous crystallographic orientations and collectively exhibit a diverse range of faceting. The nanoshells derived from similarly oriented templates do, however, appear identical to those formed on sapphire. Figure 2a,b shows a comparison of nanoshells derived from a bare and Pt-passivated template. A smoother morphology is, as expected, observed for the nanoshell derived from the passivated template, but where the surface is buckled at numerous locations. The buckling likely originates from strains formed during the initial heteroepitaxial deposition of Pt onto the Ag template which, based on lattice mismatch (Table 1), would place the Pt under tensile strain. As the underlying template is consumed in the replacement reaction, there exists the possibility for such strains to be relieved through buckling. Complete strain relaxation is, however, inhibited for the case of substrate-based nanoshells since the base of the shell is affixed to the substrate in the strained configuration. This accounts for the frequent appearance of nanoshells with edges that have torn from the substrate and curled (Figure S1a of the Supporting Information). The fact that strained nanoshells can be derived from galvanic replacement reactions could prove important since nanoparticle strain can give rise to impressive catalytic activity.[40,41]

Ag templates passivated with either Au or Pt undergo a hollowing process which is far more organized than for the case of bare templates. Figure 2c,d shows TEM images and element maps for Au-passivated Ag templates which have been reacted to varying degrees. The images show that the hollowing process proceeds through the formation of a hollow channel which first extends across the entire extent of the structure and then widens until the template is consumed. The EDS line scans and elemental color maps confirm the loss of Ag from the channels, while simultaneously showing uniform deposition of Pt over the entire template surface. Such channels, which are ⟨110⟩-directed (Figure S2 of the Supporting Information), were also observed in our previous study of the galvanic replacement of Ag templates with Au using aqueous $HAuCl_4$.[32] Pt channels are, however, unique in that (i) the channels are narrower at the stage where they first extend across the entire extent of the template and (ii) two channels running parallel to each other are often observed. Channels have also been observed for the case of bare templates, but are less common. The result suggests that the dissolution of Ag from bare templates is far more disorganized, with Ag exiting the structure from multiple openings on the template surface.

Role of Template Composition. Sacrificial templates composed of Ag, Pb, Cu, Ni, and Co were prepared on sapphire substrates in both the bare and Pt-passivated configurations. Figure 3 shows top- and tilted-view SEM images of the nanoshells obtained for Ag, Cu, Ni, and Co. The structures imaged were chosen to be of similar size and with faceting

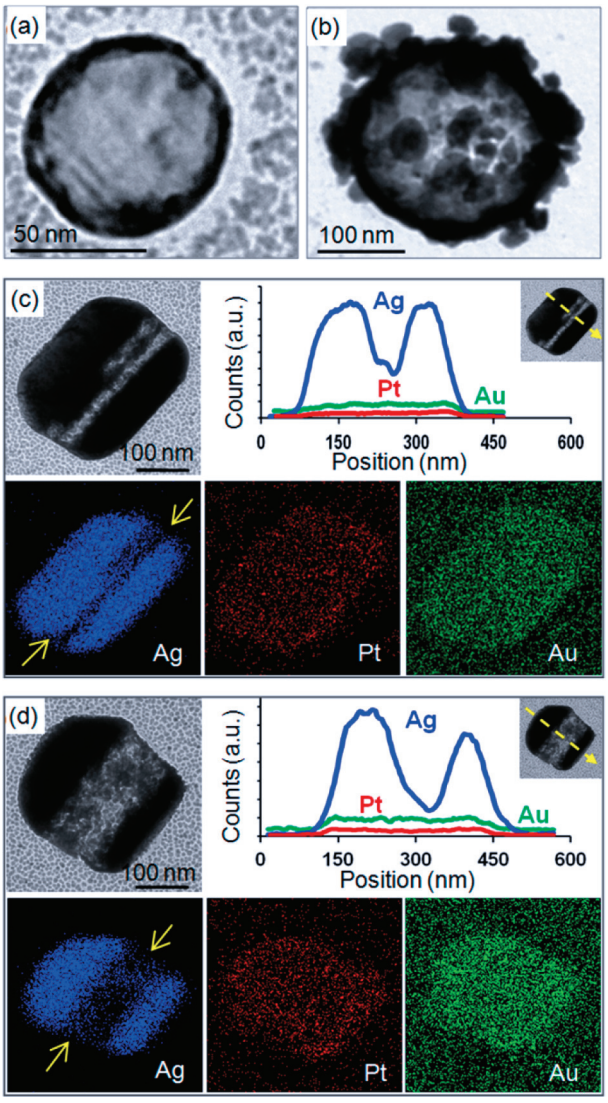

Figure 2. Images comparing nanoshells derived from (a) passivated and (b) bare Ag templates which were formed directly on Si_3N_4 support films. TEM images with corresponding line scans and elemental maps of Au-passivated templates which have undergone a galvanic replacement reaction which was halted at an (c) early stage and (d) midstage. Note that Pt evenly coats the surface as Ag exits the template in an organized manner through a highly directional channel. The smaller particles surrounding the nanoshells are remnants of the surface passivation layer.

consistent with a [111]-oriented structure. The galvanic replacement of Pb templates did not result in nanoshell formation, but instead gave rise to either (i) shriveled structures which were collapsed, wrinkled, and much smaller than the original template or (ii) structures of similar size to the starting template, but which appeared shredded and highly distorted (Figure S1b of the Supporting Information). For all template materials, the bare templates resulted in nanoshells with rough surface morphologies. In stark contrast, Pt-passivated templates yield smooth morphologies regardless of the template material utilized. In addition, the nanoshells exhibit faceting which is more pronounced than the starting templates, a result consistent with the preferential deposition of Pt on high surface energy facets. While all passivated templates yield smooth morphologies, significant differences are apparent when

dx.doi.org/10.1021/cm501418d | Chem. Mater. 2014, 26, 3340−3347

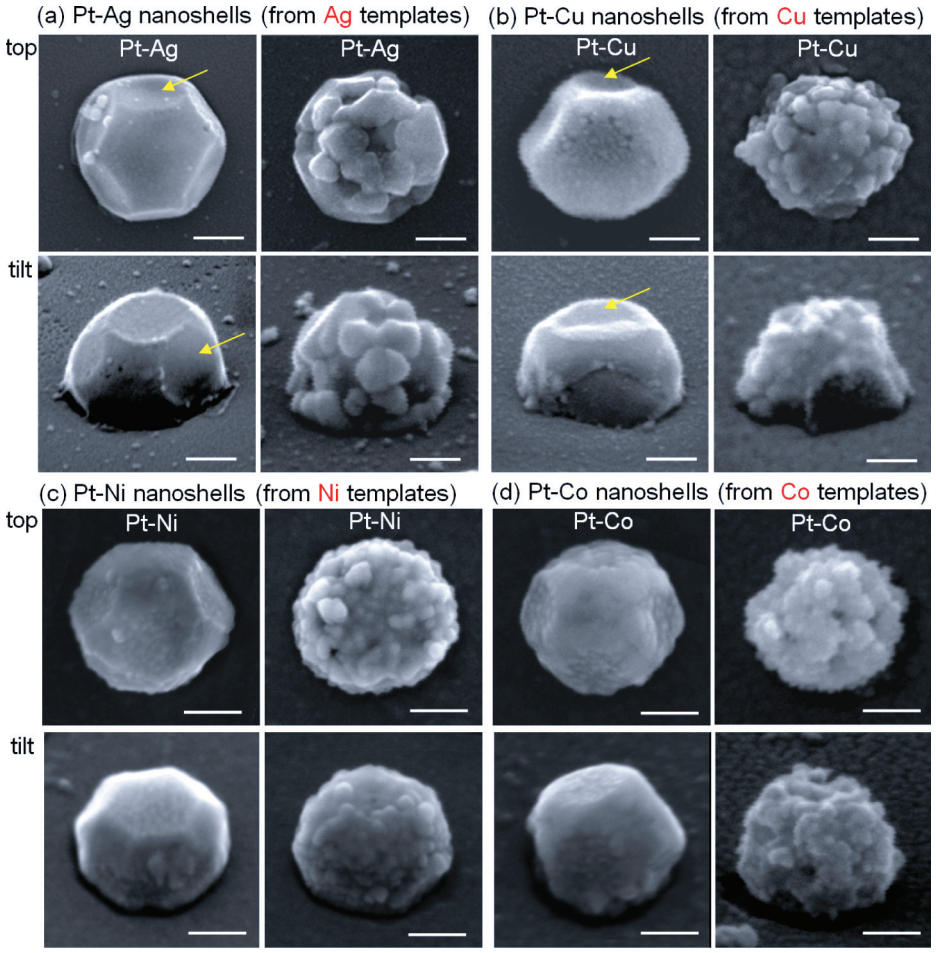

Figure 3. SEM images of nanoshells derived from Pt-passivated and bare templates for substrate-based templates assembled from (a) Ag, (b) Cu, (c) Ni, and (d) Co. Note that, in all cases, the passivated template results in a smoother surface morphology. The yellow arrows denote buckling. Scale bar is 100 nm.

comparing the nanoshells derived from the various template materials. Those derived from Cu templates often appear distorted, where in the most exaggerated cases they appear to fold or even partially collapse (Figure S1c of the Supporting Information). Such distortions are consistent with the establishment and subsequent release of compressive strains as Pt is deposited on a lattice mismatched template (Table 1) which is then consumed by the replacement reaction. Noteworthy is that these strained nanoshells never tear from the substrate at their base as is the case when Ag templates are used. The observed difference is consistent with Cu and Ag templates, giving rise to compressive and tensile strains, respectively. Pt shells when released from the underlying template will, therefore, tend to contract for the Ag case and expand for the Cu case. Pb templates behave identically to Ag, but where the much larger lattice mismatch with Pt (20.4% vs 3.5%) leads to tensile stresses which cause the nanoshell to shrivel or shred. Nanoshells derived from Ni and Co templates are expected to behave much like Cu, but show less indications of stress, a likely consequence of the fact that these shells are thicker due to the 2:1, as opposed to 4:1, replacement ratio. The hollow nature of these thicker structures was confirmed using EDS line scans (Figure S3 of the Supporting Information).

Expectations were that surface passivation would also have a significant influence on the composition of the nanoshell. Passivation not only adds extra Pt through the coating process but also should limit the number of vacancies created at the template surface during the initial stages of the replacement reaction when two (for Pb, Ni, and Co) or four (for Ag and Cu) times as many template atoms leave the surface compared to the number of Pt atoms arriving. With vacancy diffusion being the primary mechanism for alloying in the solid state, such a reduction could prove significant. This, however, is not the case when Ag or Pb templates are reacted. EDS measurements, shown in Figure 4a,b, indicate the formation of heavily alloyed nanoshells (i.e., $Pt_{0.5}Ag_{0.5}$ and $Pt_{0.6}Pb_{O.4}$) resulting from strong interdiffusion between the depositing nanoshell and the subsurface template material. In contrast, nanoshells derived from Cu templates (Figure 4c) show levels of alloying ($Pt_{0.98}Cu_{.0.02}$), with some shells showing no Cu signature. Even less interdiffusion occurs for the case of Ni and Co templates, with most of the structures showing no measurable levels of alloying (Figure 4d,e).

Mechanisms Guiding the Galvanic Replacement of Surface-Passivated Templates. The results presented define distinct and separate roles for template surface passivation layers and template composition in determining the product of the galvanic replacement reaction. An appropriately chosen passivation layer can be used to improve the nanoshell surface morphology irrespective of the composition of the underlying template material. The template composition dictates the final

dx.doi.org/10.1021/cm501418d | *Chem. Mater.* 2014, 26, 3340−3347

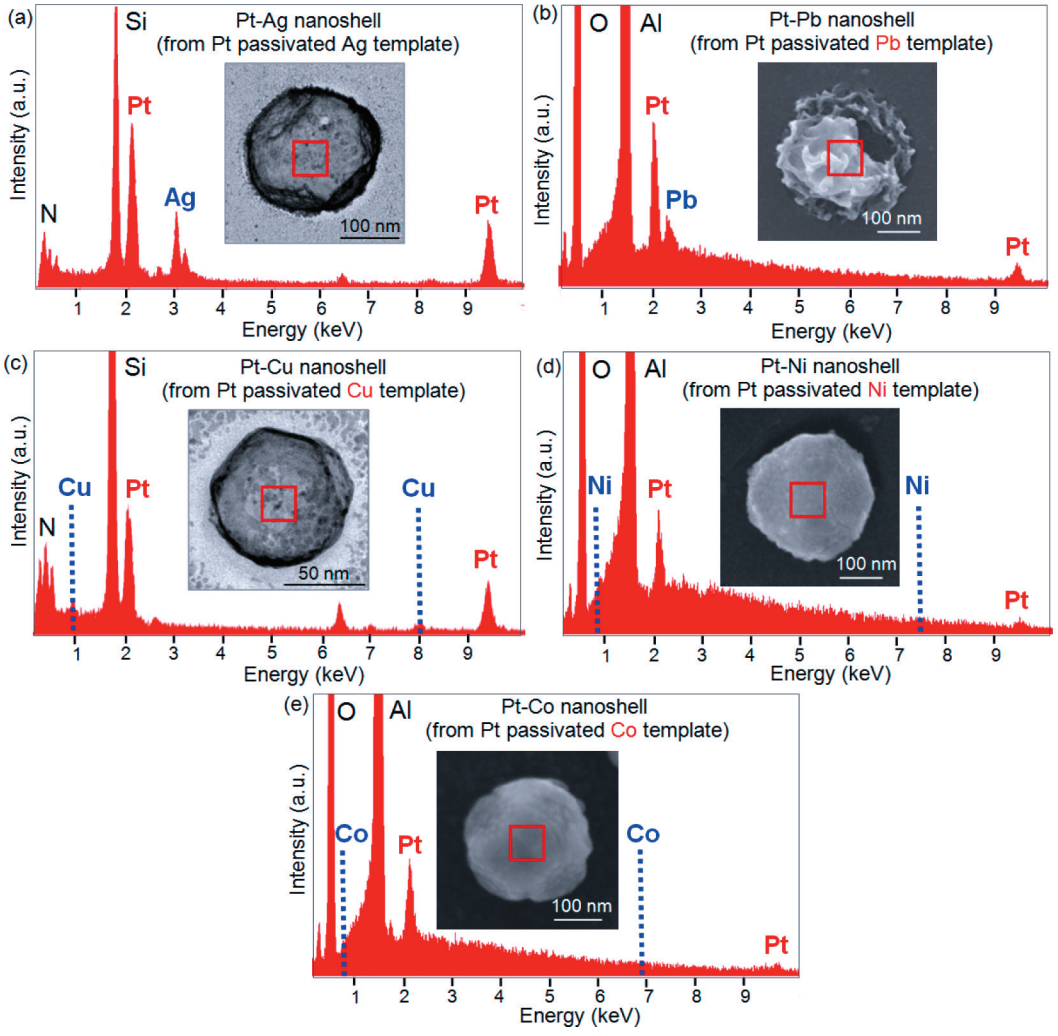

Figure 4. EDS spectra for nanoshells derived from Pt-passivated templates composed of (a) Ag, (b) Pb, (c) Cu, (d) Ni, and (e) Co. Note that high levels of alloying occur only when the nanoshells are derived from Ag or Pb templates.

composition of the nanoshell through the degree by which it alloys with Pt. On the basis of our findings, we propose mechanisms by which the nanoshell composition and surface morphology are determined by the sacrificial template. Figure 5 shows schematic representations of the proposed growth modes responsible for (i) rough nanoshells, (ii) smooth nanoshells with minimal alloying, and (iii) smooth nanoshells with a high degree of alloying. In the absence of a passivation layer (Figure 5a), the entire template surface is initially available to the replacement reaction. The rounded template presents a highly reactive surface from which the oxidized template atoms can exit the structure as Pt is deposited on its surface. The continuity and morphology of the forming nanoshell is compromised by both template pitting due to surface replacement and the inability to deposit on areas from which Ag is rapidly dissolving. The emerging nanoshell, at this point, consists of isolated islands which, as the reaction proceeds, merge to form a nanoshell consisting of many loosely connected lobes. When the template surface is passivated with Pt (Figure 5b,c), the initial stages of the replacement reaction are frustrated by the fact that subsurface Ag is not readily available. The reaction can only proceed when the passivation layer is breached. The role of this layer is, hence, to define a single opening from which dissolution occurs. The template material then exits the structure through the opening as Pt is deposited over the entire template surface. The reaction will continue until the template is consumed, but where the final nanoshell composition is determined by the number of template atoms which diffused into Pt over the course of the reaction. This diffusion process does not seem strongly related to the degree of miscibility between Pt and the template material. Ag, which has the lowest miscibility, shows the highest level of alloying. Pb, Cu, Ni, and Co all show high levels of miscibility, but only Pb shows a high degree of alloying. This suggests that the alloying process is not driven completely by thermodynamics, but is, instead, strongly influenced by kinetics. The Cu, Ni, and Co templates are, hence, unable to alloy because the kinetics of diffusion process responsible for alloying are too slow compared to the speed at which these templates are consumed. Because we see no evidence for faster template consumption for these three template materials, it follows that the diffusion process is slower. Solid-state diffusion between two materials is reliant on the exchange of vacancies. The rate of diffusion is, therefore, dependent on the number of vacancies and the activation energy associated with vacancy motion. This activation energy has been shown, both experimentally[42,43] and theoretically,[44] to be strongly influenced by elastic strains such as those imposed by lattice mismatch. The observed buckling of

dx.doi.org/10.1021/cm501418d | *Chem. Mater.* 2014, 26, 3340−3347

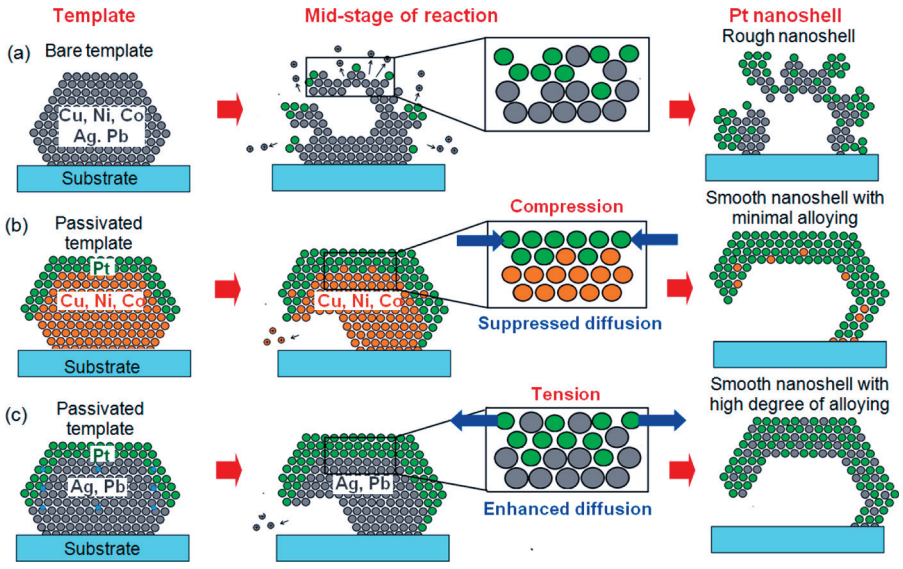

Figure 5. Schematic representations of three distinct nanoshell growth modes. (a) Highly reactive bare templates result in rough and porous nanoshells due to a disorganized replacement reaction characterized by pitting and dissolution from numerous locations on the template surface. (b) Passivated templates which place the emerging nanoshell under compressive strain (i.e., Cu, Ni, Co) leads to template dissolution from a single opening and minimal alloying due to an increase in the diffusion barrier. (c) Passivated templates which place the emerging nanoshell under tensile strain (i.e., Ag, Pb) leads to template dissolution from a single opening and a high degree of alloying due to a decrease in the diffusion barrier.

nanoshells is evidence that such strains exist. Cu, Ni, and Co are expected to place Pt under the compressive strains (Table 1) needed to impose a barrier to diffusion. In contrast, Ag and Pb templates are expected to place Pt under tensile stress, the result of which is enhanced diffusion. We, therefore, contend that templates which place the nanoshell under compressive stress (Figure 5b) will show a comparatively small amount of alloying when compared to those which place it under tensile stress (Figure 5c).

Much of the literature dedicated to Pt-based galvanic replacement reactions fits within the framework of our proposed mechanisms. The high degree of alloying observed when reacting Ag templates results from the enhanced diffusion associated with tensile stress. The rough surface morphologies arising from bare elemental templates (Ag, Cu, Ni, and Co) originates from early stage pitting and the inability to deposit on the numerous areas from which the template material is oxidizing. The smooth and continuous Pt nanostructures obtained for (i) Ag templates with an AgCl coating,[16,21] (ii) Ni templates exposed to an H_2SO_4 pretreatment,[29] (iii) Te templates reacted in ethylene glycol,[28] and (iv) Pd templates reacted in Br^{-}[30] could, in fact, all be examples of protocols which, in one form or another, passivate the template prior to reaction. If this is indeed the case, then these protocols, in conjunction with the current study, advocate an overall strategy for the design of template architectures able to promote the formation of smooth nanoshells with minimal alloying. Such templates should consist of a core−shell geometry. The core should be composed of an element which is readily oxidized and which promotes a heteroepitaxial relationship which places the depositing material under the compressive strains needed to impose a significant barrier to diffusion. The shell should (i) be inert to replacement, (ii) have a composition identical to the element being reduced onto the surface during galvanic replacement or, alternatively, be amenable to removal through selective etching following the reaction, (iii) be thin enough to promote a breach from which the core material can exit the structure as it is oxidized, and (iv) have conductivity sufficient to allow for the electron flow needed to sustain a galvanic replacement reaction between an inner anode and an outer shell cathode.

CONCLUSION

Using sacrificial templates derived from the solid-state dewetting of five different elements, we have demonstrated substrate-based galvanic replacement reactions yielding Pt nanoshells. In all cases, we were only able to form smooth continuous nanoshells when a thin passivation layer was applied to the template prior to the initiation of the replacement reaction. The ability to form smooth nanoshells irrespective of the shell composition establishes template surface passivation as the primary mode by which smooth Pt nanoshells are obtained. Such shells exhibited minimal alloying with Cu, Ni, and Co templates, but showed a high degree of alloying with Ag and Pb. We assert that nanoshell alloying is a kinetically driven process strongly dependent on heteroepitaxial strains originating from lattice mismatch between the depositing shell and underlying template material, whereby compressive strains inhibit alloying while tensile strains promote it. It is, thus, concluded that appropriately designed core−shell templates provide the clearest pathway to the synthesis of smooth continuous nanoshells with minimal alloying.

ASSOCIATED CONTENT

Supporting Information

Tables S1 and Figures S1−S3. This material is available free of charge via the Internet at http://pubs.acs.org.

AUTHOR INFORMATION

Corresponding Author

*E-mail: neretina@temple.edu.

Notes

The authors declare no competing financial interest.

■ ACKNOWLEDGMENTS

This work is funded by the NSF (DMR-1053416) CAREER Award to S.N. The authors also acknowledge the expertise of F. Monson (Technical Director, Center for Microanalysis, Imaging, Research and Training, West Chester University) and D. Dikin (Facility Manager, Nano Instrumentation Center, Temple University). The work has benefited from the facilities available through Temple University's Material Research Facility (MRF) and the Penn Regional Nanotechnology Facility. K.D.G. acknowledges support received through a Temple University Graduate Student Fellowship.

■ REFERENCES

(1) Xia, X.; Wang, Y.; Ruditskiy, A.; Xia, Y. *Adv. Mater.* **2013**, *25*, 6313.
(2) Burda, C.; Chen, X. B.; Narayanan, R.; El-Sayed, M. A. *Chem. Rev.* **2005**, *105*, 1025.
(3) Cheong, S.; Watt, J. D.; Tilley, R. D. *Nanoscale* **2010**, *2*, 2045.
(4) Kloke, A.; von Stetten, F.; Zengerle, R.; Kerzenmacher, S. *Adv. Mater.* **2011**, *23*, 4976.
(5) Du, C.; Chen, M.; Wang, W.; Tan, Q.; Xiong, K.; Yin, G. *J. Power Sources* **2013**, *240*, 630.
(6) Rycenga, M.; Cobley, C. M.; Zeng, J.; Li, W. Y.; Moran, C. H.; Zhang, Q.; Qin, D.; Xia, Y. N. *Chem. Rev.* **2011**, *111*, 3669.
(7) Jiang, X. C.; Yu, A. B. J. *Nanosci. Nanotechnol.* **2010**, *10*, 7829.
(8) Chen, H. M.; Liu, R.-S.; Lo, M.-Y.; Chang, S.-C.; Tsai, L.-D.; Peng, Y.-M.; Lee, J.-F. *J. Phys. Chem. C* **2008**, *112*, 7522.
(9) Kim, M. R.; Lee, D. K.; Jang, D.-J. *Appl. Catal., B* **2011**, *103*, 253.
(10) Chen, J.; Wiley, B.; McLellan, J.; Xiong, Y.; Li, Z.-Y.; Xia, Y. *Nano Lett.* **2005**, *5*, 2058.
(11) Bansal, V.; O'Mullane, A. P.; Bhargava, S. K. *Electrochem. Commun.* **2009**, *11*, 1639.
(12) Mahmoud, M. A.; Saira, F.; El-Sayed, M. A. *Nano Lett.* **2010**, *10*, 3764.
(13) Mahmoud, M. A.; El-Sayed, M. A. *Langmuir* **2012**, *28*, 4051.
(14) Lee, C.-L.; Tseng, C.-M. *J. Phys. Chem. C* **2008**, *112*, 13342.
(15) Seo, D.; Song, H. *J. Am. Chem. Soc.* **2009**, *131*, 18210−18211.
(16) Bi, Y.; Ye, J. *Chem. Commun.* **2010**, *46*, 1532.
(17) Shen, Y.-L.; Chen, S.-Y.; Song, J.-M.; Chen, I.-G. *Nanoscale Res. Lett.* **2012**, *7*, 245.
(18) Sławiński, G. W.; Zamborini, F. P. *Langmuir* **2007**, *23*, 10357.
(19) Chen, H. M.; Liu, R.-S.; Lo, M.-Y.; Chang, S.-C.; Tsai, L.-D.; Peng, Y.-M.; Lee, J.-F. *J. Phys. Chem. C* **2008**, *112*, 7522.
(20) Cui, C.; Gan, L.; Heggen, M.; Rudi, S.; Strasser, P. *Nat. Mater.* **2013**, *12*, 765.
(21) Zhang, W.; Yang, J.; Lu, X. *ACS Nano* **2012**, *6*, 7397.
(22) Liang, H.-P.; Zhang, H.-M.; Hu, J.-S.; Guo, Y.-G.; Wan, L.-J.; Bai, C.-L. *Angew. Chem., Int. Ed.* **2004**, *43*, 1540.
(23) Vasquez, Y.; Sra, A. K.; Schaak, R. E. *J. Am. Chem. Soc.* **2005**, *127*, 12504.
(24) Pasricha, R.; Bala, T.; Biradar, A. V.; Umbarkar, S. *Small* **2009**, *5*, 1467.
(25) Mohl, M.; Kumar, A.; Reddy, A. L. M.; Kukovecz, A.; Konya, Z.; Kiricsi, I.; Vajtai, R.; Ajayan, P. M. *J. Phys. Chem. C* **2010**, *114*, 389.
(26) Li, Q.; Xu, P.; Zhang, B.; Wu, G.; Zhao, H.; Fu, E.; Wang, H.-L. *Nanoscale* **2013**, *5*, 7395.
(27) Park, D.-Y.; Jung, H. S.; Rheem, Y.; Hangarter, C. M.; Lee, Y.-I.; Ko, J. M.; Choa, Y.-H.; Myung, N. V. *Electrochim. Acta* **2010**, *55*, 4212.
(28) Liang, H.-W.; Liu, S.; Gong, J.-Y.; Wang, S.-B.; Wang, L.; Yu, S.-H. *Adv. Mater.* **2009**, *21*, 1850.
(29) Liu, L.; Yoo, S.-H.; Park, S. *Chem. Mater.* **2010**, *22*, 2681.
(30) Zhang, H.; Jin, M.; Wang, J.; Li, W.; Camargo, P. H. C.; Kim, M. J.; Yang, D.; Xie, Z.; Xia, Y. *J. Am. Chem. Soc.* **2011**, *133*, 6078.
(31) Gilroy, K. D.; Farzinpour, P.; Sundar, A.; Tan, T.; Hughes, R. A.; Neretina, S. *Nano Res.* **2013**, *6*, 418.
(32) Gilroy, K. D.; Sundar, A.; Farzinpour, P.; Hughes, R. A.; Neretina, S. *Nano Res.* **2014**, *7*, 365.
(33) Thompson, C. V. *Annu. Rev. Mater. Res.* **2012**, *42*, 399.
(34) Farzinpour, P.; Sundar, A.; Gilroy, K. D.; Eskin, Z. E.; Hughes, R. A.; Neretina, S. *Nanoscale* **2013**, *5*, 1929.
(35) Farzinpour, P.; Sundar, A.; Gilroy, K. D.; Eskin, Z. E.; Hughes, R. A.; Neretina, S. *Nanotechnology* **2012**, *23*, 495604.
(36) Harris, D. C. *Quantitative Chemical Analysis*, 7th ed.; W. H. Freeman and Co.: New York, 2006; pp AP20−AP27.
(37) Li, D. G.; Wang, C.; Tripkovic, D.; Sun, S. H.; Markovic, N. M.; Stamenkovic, V. R. *ACS Catal.* **2012**, *2*, 1358.
(38) Lee, H.; Habas, S. E.; Kweskin, S.; Butcher, D.; Somorjal, G. A.; Yang, P. D. *Angew. Chem., Int. Ed.* **2006**, *45*, 7824.
(39) Henry, C. R. *Prog. Surf. Sci.* **2005**, *80*, 92.
(40) Wang, J. X.; Ma, C.; Choi, Y.; Su, D.; Zhu, Y.; Liu, P.; Si, R.; Vukmirovic, M. B.; Zhang, Y.; Adzic, R. R. *J. Am. Chem. Soc.* **2011**, *133*, 13551.
(41) Strasser, P.; Koh, S.; Anniyev, T.; Greeley, J.; More, K.; Yu, C. F. Z.; Liu, C.; Kaya, S.; Nordlund, D.; Ogasawara, H.; Toney, M. F.; Nilsson, A. *Nat. Chem.* **2010**, *2*, 454.
(42) Dickerson, R. H.; Lowell, R. C.; Tomizuka, C. T. *Phys. Rev.* **1965**, *137*, A613.
(43) Lang, Ch.; Schmitz, G. *Mater. Sci. Eng., A* **2003**, *353*, 119.
(44) Jang, J.-W.; Kwon, J.; Lee, B.-J. *Scr. Mater.* **2010**, *63*, 39.